J. Astrophys. Astr. (2023) 44:49
https://doi.org/10.1007/s12036-023-09943-x

Evolution of weak discontinuity waves in non-ideal interstellar environments

SHWETA[1,*], RAHUL KUMAR CHATURVEDI[1,2], SHOBHIT KUMAR SRIVASTAVA[1] and L. P. SINGH[1]

[1]Department of Mathematical Sciences, Indian Institute of Technology, Banaras Hindu University, Varanasi 221005, India.
[2]School of Advanced Sciences and Languages, VIT Bhopal University, Bhopal 466114, India.
*Corresponding author. E-mail: shweta.rs.mat19@itbhu.ac.in

MS received 12 September 2022; accepted 23 February 2023

Abstract. A systematic method is used to study the problem of propagation of planar, cylindrically symmetric and spherically symmetric shock waves of the one-dimensional motion of an inviscid, self-gravitating, non-ideal interstellar gas cloud. The analytic solution of the problem is resolved, which specifies non-linear behavior in the physical plane. The transport equation, which describes the evolution of weak discontinuity in non-ideal gas is derived. It is observed that the nature of the solution completely depends on the net volumetric cooling rate and self-gravitating parameter. It is observed that an increase in the value of self-gravitating parameter results in delay of process of shock formation and shock forms early when heating dominates cooling in the system. Also, expansive waves take less time to decay in planar geometry as compared to cylindrical and spherical geometries and compressive waves take more time to develop shocks for cylindrical and spherical geometries as compared to planar geometry.

Keywords. Hyperbolic system—shock wave—interstellar gas clouds—non-ideal gas.

1. Introduction

Most of the physical phenomena occurring in compressible fluids are non-linear, which may be modeled mathematically in the form of non-linear partial differential equations (PDEs). Such PDEs contribute to many problems of supersonic flows, plasma flows, interstellar flows, aerospace science, space research, astrophysics and many more. Laws of mechanics and thermodynamics forms the theoretical basis of gas dynamics. Shock waves arise due to sudden changes in the flow variables. Their study has great significance in innumerable fields and in recent years, its practical importance has risen due to its specific applications in astrometry, uranology, nuclear physics, geology, seismology and their applications to the satellite's motion. Due to energetic events like the collision of clouds, stellar winds, powerful and luminous stellar explosion, supernova blast, rapid crashes between interstellar gas clusters, remarkably high rate of star formation, etc., the shock waves become usual in the interstellar medium. The authors (Lax 1957; Chen & Gurtin 1971; Shyam *et al.* 1981; Pandey 1991; Courant & Friedrichs 1999; Shah *et al.* 2010; Modelevsky & Sari 2021; Chaturvedi *et al.* 2022) have used several analytical approaches to study the phenomena of shock formation, diverging and converging shock waves, growth and deteriorating behavior of shocks and propagation of shock waves in several regimes. Nath & Singh (2019) studied the evolution of cylindrical shocks with isothermal flow condition using power series method. Maslov & Tsupin (1980) proposed a new method to depict the geometry of movement of shocks in an isentropic gas using the universal method of difference schemes. Higashino (1983) studied non-uniform propagation of flow of blast wave and shock tube problem using Hartree's method in dusty gas cloud. Nath (2020) investigated explosion problems for cylindrical and spherical symmetry cases. Singh & Arora (2021b) have studied one-dimensional shocks with the help of infinite hierarchy of the transport equation and truncation approximation method in the presence of radiating gas. The kinematics of cylindrical shocks in rotationally axisymmetric non-ideal gas was studied by Nath *et al.* (2019). To examine evolution of shocks, Singh & Arora (2021a) used the power series method and discussed the impact of shock Cowling number and

Published online: 20 May 2023

non-ideal parameter on flow variables. Various studies on other facts about shocks are done by many authors in the literature (see Singh *et al.* 2016; Gupta *et al.* 2020; Srivastava *et al.* 2020b, 2021).

A commonly occurring situation for the problems related to shocks is lower temperatures and high pressures, where ideal gas assumptions are no longer valid. Then, the model of non-ideal gas is the prevailing substitute model for it. Roberts & Wu (1996) and Wu & Roberts (1993) adopted the van der Waals model and discussed the theory of shock waves of sonoluminescence. Gupta *et al.* (2022) investigated one-dimensional unsteady cylindrical shocks in non-ideal gas with isothermal flow. Sahu (2022) considered gravity field, variable magnetic field, radiation flux and thermal conduction for self-similar flow solution originated through traveling piston in non-ideal gas filled with dust. Nath (2022) proposed evolution of shocks of micro-sized dust particles with monochromatic radiation. Arora & Siddiqui (2013) have derived the transport equation to discuss the evolutionary behavior of planar, cylindrical and spherical weak shocks in the non-ideal medium. Arora *et al.* (2012) have worked on the collapse of imploding cylindrically and spherically symmetric shocks to obtain solutions of shock waves of strong strength in non-ideal gas. Related articles for the study of shock wave solutions in non-ideal gas dynamics (see Pandey & Sharma 2009; Nath & Vishwakarma 2016; Bira *et al.* 2018; Singh *et al.* 2020a). Various phenomena in space research and astronomical physics, including the gravitational collapse in the interstellar medium, are significant due to the description of star-forming regions. Hence, study of collapse of a self-gravitating interstellar gas cloud in the spiral arms of the Galaxy has shifted the attention of astrophysicists as they had an interest in patterns of stellar systems, stars and supernova explosions. The study of interstellar gas dynamics is important to understand the energy budget, structure and evolution of the interstellar medium. Interstellar medium is intermittently disturbed by violent events, which results in major rise in pressure and with its increase, the disturbed area will expand. When rise in pressure exceeds a minimum value, a 'shock front' is developed and the flow in neighboring front is referred as 'shock wave'. The problem of interstellar gas clouds with shock waves has been addressed by various authors. Zeidan *et al.* (2022) discussed the interaction of accelerating and shock waves at stellar surfaces using Lie's method. Jena & Mittal (2021) investigated the application of singular surface theory using the method of Lie group transformation. Gupta & Jena (2018) have studied the propagation of strong shocks using the kinematics of one-dimensional shocks and also explored the nature of heating–cooling functions on shocks. Bisnovatyi-Kogan & Silich (1995) introduced numerical and analytical methods of evolutionary shocks in non-homogeneous interstellar medium. Bedogni & Woodward (1990) had provided a detailed description of the interaction of interstellar gas cloud with the shock wave. Heathcote & Brand (1983) have discussed the interaction of supernova blast with the interstellar cloud. Ferraioli *et al.* (1978) had studied the gravitational collapse of interstellar gas cloud using the propagating theory of wave, and analyzed the role of heating–cooling functions in the formation of shock wave. Sharma & Arora (2021) have studied the interconnection between acceleration wave and characteristic shock and observed the effect of non-ideal parameters on acceleration wave amplitude. In an interstellar dusty gas cloud, the evolution of weak and strong shocks is analyzed by Chauhan & Arora (2021). Also, the effect of heating–cooling parameters is shown graphically. Singh *et al.* (2020b) have studied the effect of non-idealness on evolutionary behavior of shocks using compatibility conditions and truncation procedure. The formation of shocks in a gravitating atmosphere is discussed by Chauhan & Arora (2021).

In the present work, the evolution of weak discontinuities has been studied using the method of characteristics for one-dimensional motion of an inviscid, self-gravitating interstellar medium. In continuum mechanics, the weak discontinuity waves are known as acceleration waves. They have continuous solution and occur in the solution's derivative along with the characteristics. Weak discontinuities occur in numerous media, and we observe that their amplitudes follow the subsequent differential equation:

$$\frac{dY}{dt} = -\alpha Y + \delta Y^2, \quad 0 \leq t \leq \infty,$$

presents Bernoulli equation, where Y denotes the amplitudes of the discontinuity. Generally, α and δ are the functions of time t. The solution to Bernoulli's equation is required for the complete analysis of the flow profile of weak discontinuities. As we are able to obtain the amplitude of the weak discontinuity closely without any approximations, despite working with a completely nonlinear system, this is the main reason why weak discontinuities are especially useful. The evolution equation for planar and non-planar shocks is derived in interstellar gas clouds. Majorally, our motive is to study how acceleration waves are steepened or flattened after the formation of shock wave and to discuss the impact of cooling–heating function and self-gravitating parameter on the nature of solution. As per our knowledge, the study of propagation of shock wave in interstellar gas clouds under the impact of van der Waals gas have not been investigated yet by any researcher, whereas it has wide application in astronomical problems, star formation, cloud collapse phenomena, formation of stellar systems and in many more problems (see Ferraioli & Virgopia 1975; Disney *et al.* 1968; Gupta & Jena 2018).

The description of this paper is outlined as follows: The governing system of equations and characteristic curves that represent the wave propagation is introduced in Section 2. In Section 3, characteristic variables are introduced and we obtain solution of acceleration waves to investigate the shock formation process. Section 4 contains a detailed analysis of various parameter effects on the formation and distortion of shocks. Section 5 contains the conclusions of this study.

2. Wave propagation

The basic equations governing the one-dimensional flow with inviscid, self-gravitating and interstellar gas clouds, may be given by Ferraioli *et al.* (1978), Gupta & Jena (2018) and Singh *et al.* (2020b):

$$\begin{aligned}
&\frac{\partial \rho}{\partial t} + u\frac{\partial \rho}{\partial x} + \rho\frac{\partial u}{\partial x} + \frac{m\rho u}{x} = 0,\\
&\rho\left(\frac{\partial u}{\partial t} + u\frac{\partial u}{\partial x}\right) + \frac{\partial p}{\partial x} = g,\\
&\frac{\partial p}{\partial t} + u\frac{\partial p}{\partial x} + \rho a^2\left(\frac{\partial u}{\partial x} + \frac{mu}{x}\right)\\
&\quad = \frac{-(\gamma-1)\rho L(p,\rho)}{(1-b\rho)},\\
&\frac{\partial g}{\partial t} + u\frac{\partial g}{\partial x} = -\frac{mgu}{x}.
\end{aligned} \tag{1}$$

Here, $m = 0, 1, 2$ correspond to planar, cylindrically symmetric and spherically symmetric flows, respectively. The radial distance taken from the origin, time, density, pressure, acceleration due to gravity, van der Waals gas volume, ratio of specific heat at constant pressure to specific heat at constant volume, velocity and the net volumetric cooling rate, which have been introduced to take into account some energy loss and gain mechanism are denoted by $x, t, \rho, p, g, b, \gamma, u$ and $L(p, \rho)$, respectively. An equilibrium state for heating/cooling is supposed with $L = 0$, for the initial condition, i.e., no net gain or loss of energy. Positive or negative values of $L(p, \rho)$ represent the cooling or heating of the non-ideal interstellar medium. The sound speed, a is defined as:

$$a = \sqrt{\frac{\gamma p}{(1-\bar{b})\rho}}, \quad \text{here } \bar{b} = b\rho.$$

Since we are mainly focused on the dynamical aspects of the problem, our function $L(p, \rho)$ does not take into account sophisticated chemistry, as it is a linear combination of the following seven processes (Hunter 1969):

$$\begin{aligned}
L &= A_{ei} + A_g + A_{H_2} - B_{\mathrm{CR}} - B_{ph}\\
&\quad + A_H + C \quad (\text{erg cm}^3\ \text{s}^{-1}),
\end{aligned}$$

where

$$\begin{aligned}
A_{ei} &= \frac{n_H * n_e}{\sqrt{T} * 10^{23}}(64 \times 10^{-2} e^{-92/T}\\
&\quad + 17 \times 10^{-1} e^{-554/T} + 64 \times 10^{-1} e^{-413/T}\\
&\quad + 22 \times 10^{-1} e^{-961/T}),\\
&\quad \text{(ionic cooling)},\\
A_g &= \begin{cases} 137 \times 10^{-31} \epsilon n_H * n_H * T^{1/2}, \ (T > 180^\circ\ \mathrm{K})\\ 733 \times 10^{-34} \epsilon n_H * n_H * T^{1/2} * (T - T_g),\\ (T \le 180^\circ\ \mathrm{K}), \ \text{(inelastic collisions)}\\ \text{or}\\ 0, \ \text{(elastic collisions)}, \end{cases}\\
A_{H_2} &= 845 \times 10^{-26} n_{H_2} e^{-502/T}\\
&\quad * \left\{1 + \frac{42}{n_H T^{1/2}(1 + 0.1 n_{H_2}/n_H)}\right\}^{-1},\\
&\quad (H_2 \text{ cooling})\\
B_{CR} &= 16 \times 10^{-12} F n_H \left(1 + 2\frac{n_{H_2}}{n_H}\right)\\
&\quad \text{(heating of cosmic ray)},\\
B_{ph} &= 482 \times 10^{-28} n_H n_e T^{0.6548}\\
&\quad \text{(heating of photo-ionization)},\\
A_H &= 3 \times 10^{-24} * T^{-1/2} e^{-227/T} n_H * n_e\\
&\quad \text{(cooling of hydrogen atom)},\\
C &= -38 \times 10^{-30} * T^{-1/2} n_H * n_H e^{-23.6/T}\\
&\quad \text{(other atomic cooling processes)}.
\end{aligned}$$

Here, n_g, n_H and n_e denote the grain, hydrogen, and electron number density, respectively. F and T_g denotes cosmic ray flux and temperature of the grains and ϵ is the free parameter.

Equation of state for non-ideal gas is:

$$p = \frac{\rho R T}{(1-b\rho)}, \tag{2}$$

Here, R and T represents the gas constant and temperature, respectively. We can write Equation (1) as follows:

$$U_t + AU_x + B = 0, \tag{3}$$

where U is 4×1 ordered column vectors and A, B are 4×4 ordered matrix, shown below:

$$U = \begin{pmatrix} \rho \\ u \\ p \\ g \end{pmatrix}, \quad B = \begin{pmatrix} \frac{m\rho u}{x} \\ -g \\ \frac{m\rho a^2 u}{x} + \frac{(\gamma-1)\rho L}{1-b\rho} \\ \frac{mgu}{x} \end{pmatrix}$$

and

$$A = \begin{pmatrix} u & \rho & 0 & 0 \\ 0 & u & 1/\rho & 0 \\ 0 & \rho a^2 & u & 0 \\ 0 & 0 & 0 & u \end{pmatrix}.$$

The function $U(x, t)$ satisfying Equation (3), is continuous everywhere, but its derivatives U_t and U_x may suffer finite jump along the characteristic curve $C(t)$ and it is called weak discontinuity. Now, along $C(t)$, we get:

$$\frac{\partial}{\partial t}[U] = [U_t] + \frac{dC(t)}{dt}[U_x], \tag{4}$$

where $\partial/\partial t$ denotes time derivative t. Since U is a continuous function, therefore $[U] = 0$.

Taking jump in (3) and combining (4) with $[U] = 0$, we obtain:

$$\left(A - \frac{dC}{dt}I\right)[U_x] = 0. \tag{5}$$

From (5), we can see that the characteristic speed of propagation dC/dt is an eigenvalue of the matrix A along the characteristic curve $C(t)$. The characteristic curves for (3), are as follows:

$$\frac{dx}{dt} = u \tag{6}$$

and

$$\frac{dx}{dt} = u \pm a, \tag{7}$$

represent the path of the particle and wave propagation in $\pm x$ direction, respectively.

3. Acceleration waves solution

We introduce ξ and ϕ as two characteristic variables and use them as a frame of reference, where ξ and ϕ are particle tag and wave tag, respectively, with ξ being constant over the particle path $dx/dt = u$ and ϕ being constant across the characteristic $dx/dt = u + a$. So, the particle tag ξ can be marked as $\xi = t^*$ if the characteristic wavefront passes through the particle at time t^*, and the wave tag ϕ can be written as $\phi = t'$ if the outgoing wave is formed at time t'.

Thus, for each pair (ϕ, ξ), we can get a pair (x, t) as $x = x(\phi, \xi)$, $t = t(\phi, \xi)$, such that ϕ and ξ satisfies

$$x_\phi = ut_\phi, \quad x_\xi = (u + a)t_\xi. \tag{8}$$

With the help of (8), we can transform U_t and U_x as:

$$U_t = \frac{U_\xi x_\phi - U_\phi x_\xi}{J}, \quad U_x = \frac{U_\phi t_\xi - U_\xi t_\phi}{J}, \tag{9}$$

where $J = (\partial(x, t)/\partial(\phi, \xi)) = -Ct_\phi t_\xi$, which is the Jacobian of transformation.

Using (9) in (1) we get:

$$a\rho_\phi t_\xi - \rho\left(u_\phi t_\xi - u_\xi t_\phi - \frac{muat_\phi t_\xi}{x}\right) = 0, \tag{10}$$

$$a\rho u_\phi t_\xi - p_\phi t_\xi + p_\xi t_\phi = ga\rho t_\phi t_\xi, \tag{11}$$

$$ap_\phi t_\xi - \rho a^2\left(u_\phi t_\xi - u_\xi t_\phi - \frac{muat_\phi t_\xi}{x}\right) = \frac{-(\gamma - 1)\rho L(\rho, p)at_\xi t_\phi}{1 - b\rho}, \tag{12}$$

$$g_\phi = -\frac{mgut_\phi}{x}. \tag{13}$$

Using Equations (11)–(13) in (10), we obtain:

$$p_\xi - ga\rho t_\xi + \rho au_\xi + \frac{m\rho a^2 ut_\xi}{x} = \frac{-(\gamma - 1)\rho L(\rho, p)t_\xi}{1 - b\rho}. \tag{14}$$

The boundary conditions at $\phi = 0$ are:

$$[\rho] = 0,\ [u] = 0,\ [p] = 0,\ [g] = 0,\ [L] = 0,\ t = \xi. \tag{15}$$

Since the flow ahead of wave is homogeneous and at rest, we observe from (15):

$$p_\xi = 0,\ u_\xi = 0,\ \rho_\xi = 0,\ L_\xi = 0,\ g_\xi = 0$$

and

$$t_\xi = 1 \quad \text{at} \quad \phi = 0. \tag{16}$$

At $\phi = 0$, using (15) and (16) in (13), (11) and (8), we get:

$$\rho_\phi = \left(\frac{\rho_0}{a_0}\right)u_\phi, \tag{17}$$

$$p_\phi = \rho_0 a_0 u_\phi, \tag{18}$$

$$x_\phi = 0,\ x_\xi = a_0. \tag{19}$$

The flow variables estimated ahead of the wave are indicated by the subscript '0'. Using (16) in (9), we get:

$$\left[\frac{\partial u}{\partial x}\right] = X = -\frac{u_\phi}{a_0 t_\phi}, \text{ at } \phi = 0, \tag{20}$$

where X is amplitude of weak discontinuity waves at $\phi = 0$.

Next, we will determine the dependence of u_ϕ and t_ϕ on time. Differentiating (8), (14) and (18) with respect to ϕ and ξ, at $\phi = 0$, we get:

$$\frac{t_{\phi\xi}}{t_\phi} = \frac{\gamma+1}{2(1-\bar{b})}X, \tag{21}$$

$$\frac{u_{\phi\xi}}{t_\phi} = \frac{a_0}{2}\frac{\gamma-1}{a_0^2(1-\bar{b})^2} \times \left(\frac{(1-\gamma)}{2}L_0 + (L_{\rho_0} + a_0^2 L_{p_0})\rho_0(1-\bar{b})\right) \times \frac{g_0(\gamma-1)}{2a_0(1-\bar{b})} + \frac{ma_0}{\xi}, \tag{22}$$

where the L_{ρ_0} and L_{p_0} quantities represent partial differentiation of L with respect to ρ and p, respectively. The subscript 'zero' denotes physical quantities ahead of the shock.

Differentiating (20) with respect to ξ and using (21) and (22), we get:

$$\frac{dX}{d\xi} + \left(\frac{\gamma-1}{2(1-\bar{b})a_0^2}\left(\left(\frac{1-\gamma}{2}\right)L_0 + (L_{\rho_0} + a_0^2 L_{p_0}) \times \rho_0(1-\bar{b})\right) + \frac{g_0(\gamma+1)}{4a_0(1-\bar{b})} + \frac{ma_0}{2\xi}\right)X + \left(\frac{\gamma+1}{2(1-\bar{b})}\right)X^2 = 0, \text{ at } \phi = 0. \tag{23}$$

Now, we introduce some non-dimensional quantities given as:

$$\chi = \frac{X}{X^*}, \ \psi = \frac{\xi - \xi^*}{2\xi^*} \text{ and } \delta = X^*\xi^*. \tag{24}$$

Here, δ, χ and ψ are the initial disturbance, wave amplitude and time, respectively. The superscript '*' has been used to denote the parameter's value at $t = t^*$.

Considering Equation (24), Equation (23) can be reduced to the following dimensionless form:

$$\frac{d\chi}{d\psi} + \left(\frac{\overline{L_0} + \overline{g_0}}{(1-\bar{b})} + \frac{m}{2\psi+1}\right)\chi + \frac{\delta(\gamma+1)}{(1-\bar{b})}\chi^2 = 0, \text{ at } \phi = 0. \tag{25}$$

where

$$\overline{L_0} = \frac{(\gamma-1)}{a_0^2}\left(\frac{(1-\gamma)L_0}{1-\bar{b}}\right) + (L_{\rho_0} + a_0^2 L_{p_0})\xi^*, \tag{26}$$

$$\overline{g_0} = \frac{(\gamma+1)g_0\xi^*}{2a_0} \tag{27}$$

$\overline{L_0}$ and $\overline{g_0}$ denotes net volumetric cooling rate and self gravitating parameter, respectively.

The solution of Equation (25) is:

$$\chi = \left\{(2\psi+1)^{\frac{m}{2}} e^{\left(\frac{R_0}{(1-\bar{b})}\right)\psi}\left(1 + \left(\frac{(\gamma+1)\delta}{(1-\bar{b})}J(\psi)\right)\right)\right\}^{-1}, \tag{28}$$

where

$$J(\psi) = \int_0^\psi \frac{-e^{\left(\frac{\overline{L_0}+\overline{g_0}}{(1-\bar{b})}\right)s}}{(2s+1)^{\frac{m}{2}}}ds.$$

From Equations (20) and (28), it is clear that for the formation of shock, we must have $t_\phi = 0$, i.e.,

$$1 + \left(\frac{(\gamma+1)\delta}{(1-\bar{b})}J(\psi)\right) = 0. \tag{29}$$

The function $J(\psi)$ plays a significant role in the breakdown of characteristic solution. From (29), it is clear that the compressive waves ($\delta < 0$) end into the shock waves.

4. Growth and decay of acceleration wave

We now investigate the behavior of the earlier obtained solution and examine the effect of parameters on the formation and deformation of the shocks by considering three cases for three different values of m. In computations, numerical values used are $\gamma = 1.67$ (Ogino *et al.* 1999), $\delta = -1.5$ or 0.5, $\bar{b} = 0.3$ (Chaturvedi *et al.* 2019; Srivastava *et al.* 2020a). Using the computational package Mathematica, all the computations are performed.

Case I. Planar flow (*m* = 0):
Placing $m = 0$ in (28), we obtain the solution of (25) as:

$$X = \frac{X^*}{e^{\left(\frac{\overline{L_0}+\overline{g_0}}{(1-\bar{b})}\right)\psi}\left(1 + \left(\frac{(\gamma+1)\delta}{(1-\bar{b})}J(\psi)\right)\right)}, \tag{30}$$

where

$$J(\psi) = \int_0^\psi -e^{\left(\frac{\overline{L_0}+\overline{g_0}}{(1-\bar{b})}\right)s}ds.$$

Figure 1 represents the solution curve for compressive wave, exhibiting shock formation and increase in the value of self gravitating parameter results in delay in the formation of shocks. It is clear from graph that shock forms early in case of heating function effect in

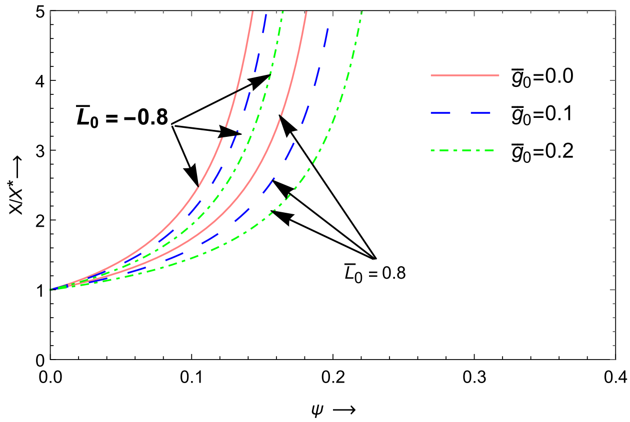

Figure 1. Effect of self gravitating parameter $\overline{g_0}$ for $\delta < 0$ with $\gamma = 1.67$, $\delta = -1.5$, $m = 0$ (planar case) and $\bar{b} = 0.3$.

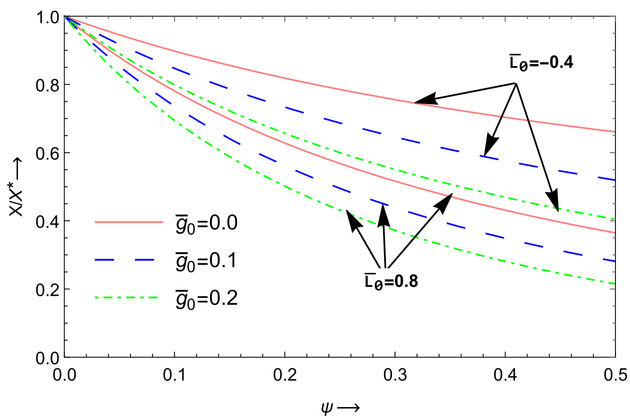

Figure 2. Effect of self gravitating parameter $\overline{g_0}$ for $\delta > 0$ with $\gamma = 1.67$, $\delta = 0.5$, $m = 0$ (planar case) and $\bar{b} = 0.3$.

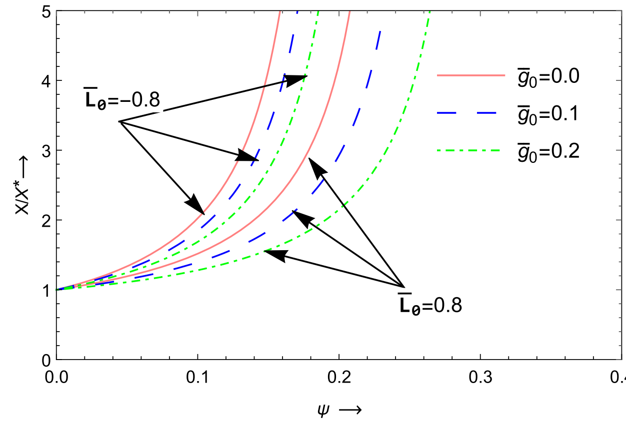

Figure 3. Effect of self gravitating parameter $\overline{g_0}$ for $\delta < 0$ with $\gamma = 1.67$, $\delta = -1.5$, $m = 1$ (cylindrical case) and $\bar{b} = 0.3$.

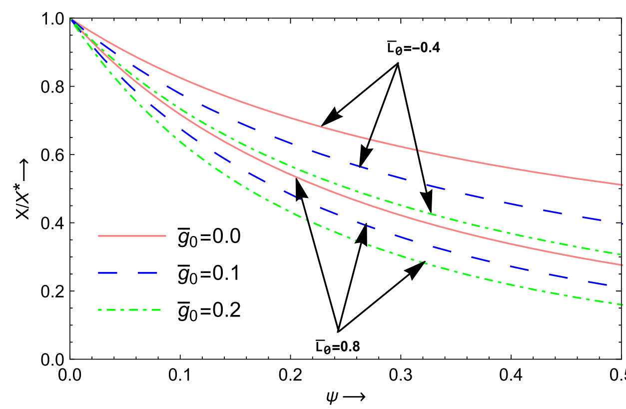

Figure 4. Effect of self gravitating field $\overline{g_0}$ for $\delta > 0$ with $\gamma = 1.67$, $\delta = 0.5$, $m = 1$ (cylindrical case) and $\bar{b} = 0.2$.

comparison to cooling function effect, but it decelerates with rise in $\overline{g_0}$. Figure 2 shows expansive wave solution curves, which clearly depict that they do not exhibit the shock formation, but decays out. With rise in $\overline{g_0}$, decay rate of propagation increases and the effect of cooling function causes to decay faster in comparison to heating function effect.

Case II. Cylindrically symmetric flow (*m* = 1): Placing $m = 1$ in (28), we obtain solution of (25) as:

$$X = \frac{X^*}{(2\psi+1)^{1/2} e^{\left(\frac{\overline{L_0}+\overline{g_0}}{(1-\bar{b})}\right)\psi} \left(1 + \left(\frac{(\gamma+1)\delta}{(1-\bar{b})} J(\psi)\right)\right)}, \tag{31}$$

where

$$J(\psi) = \int_0^{\psi} \frac{-e^{\left(\frac{\overline{L_0}+\overline{g_0}}{(1-\bar{b})}\right)s}}{(2\psi+1)^{1/2}} ds.$$

In this case, the nature of solution curves is more or less the same as that of those for planar flow. Figure 3 displays shock formation and with rise in $\overline{g_0}$, there is delay in formation of shocks. The growth rate of the compressive wave is lower in case of cooling function effect than that of heating gas cloud effect ($\overline{L_0} < 0$). Figure 4 depicts the decay rate of propagation of the expansive wave that enhances. It can be seen from the graph that the decay rate of the expansive wave is higher in the case of a cooling gas cloud, i.e., $\overline{L_0} > 0$ than that of heating gas cloud effects ($\overline{L_0} < 0$).

Figure 5 depicts compressive wave's growth behavior and with rise in $\overline{L_0}$, there is delay in formation of shock. The growth rate is very slow in the case of cooling of gas cloud $\overline{L_0} > 0$ as compared to heating of gas cloud $\overline{L_0} < 0$. Figure 6 shows the decay rate of expansive wave, which clearly depicts that it does not exhibit the shock formation and with rise in $\overline{L_0}$, the decay rate of the expansive wave rises. The decay rate is more in cooling gas cloud as compared to heating gas cloud.

Figure 7 depicts the impact of $\bar{b}$ and rise in its values results in increase in the formation of shock. Figure 8

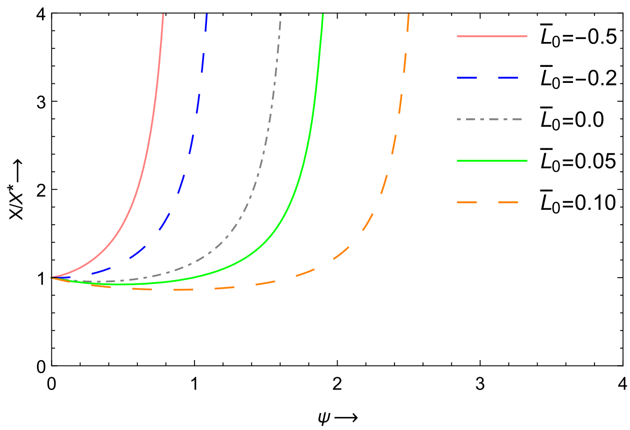

Figure 5. Effect of net volumetric cooling rate $\overline{L_0}$ for $\delta < 0$ with $\delta = -0.5$, $\gamma = 1.67$, $m = 1$ (cylindrical case) and $\bar{b} = 0.3$.

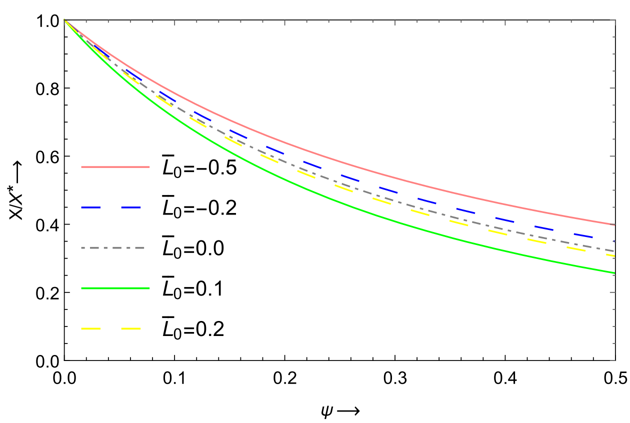

Figure 6. Effect of net volumetric cooling rate $\overline{L_0}$ for $\delta > 0$ with $\delta = 0.5$, $\gamma = 1.67$, $m = 1$ (cylindrical case) and $\bar{b} = 0.3$.

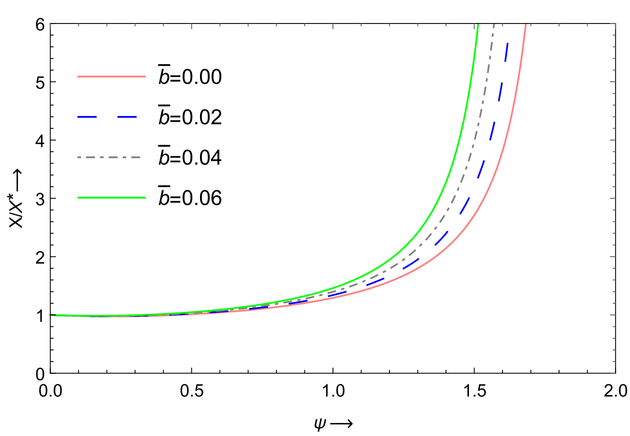

Figure 7. Effect of non-ideal parameter $\bar{b}$ for $\delta < 0$ with $\overline{L_0} = 0.4$, $\overline{g_0} = 0.2$, $m = 1$ (cylindrical case) and $\delta = -0.5$.

displays the decay rate of the expansive wave, which increases with rise in $\bar{b}$, but the increase is significantly low.

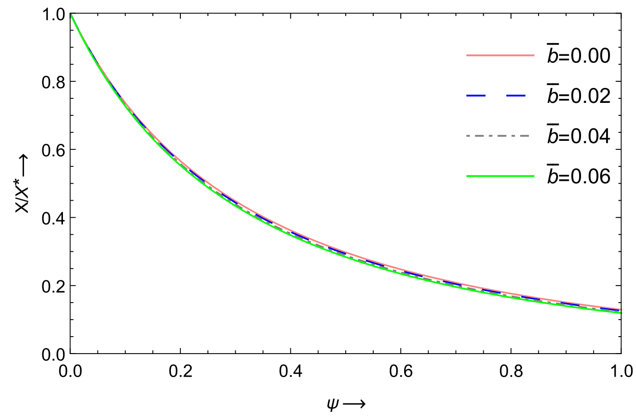

Figure 8. Effect of non-ideal parameter $\bar{b}$ for $\delta > 0$ with $\overline{L_0} = 0.2$, $\overline{g_0} = 0.8$, $m = 1$ (cylindrical case) and $\delta = 0.5$.

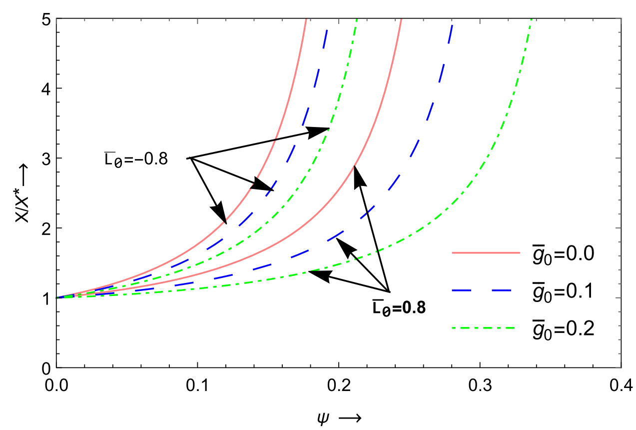

Figure 9. Effect of self gravitating parameter $\overline{g_0}$ for $\delta < 0$ with $\gamma = 1.67$, $\delta = -1.5$, $m = 2$ (spherical case) and $\bar{b} = 0.3$.

Case III. Spherically symmetric flow (*m* = 2): Placing $m = 2$ in (28), we obtain the solution of (25) as:

$$X = \frac{X^*}{(2\psi + 1) e^{\left(\frac{\overline{L_0} + \overline{g_0}}{(1-\bar{b})}\right)\psi} \left(1 + \left(\frac{(\gamma+1)\delta}{(1-\bar{b})} J(\psi)\right)\right)}, \quad (32)$$

where

$$J(\psi) = \int_0^{\psi} \frac{-e^{\left(\frac{\overline{L_0} + \overline{g_0}}{(1-\bar{b})}\right)s}}{(2\psi + 1)} ds.$$

The nature of the solution curves in this case is comparable to those for planar and cylindrically symmetric flow cases, which is evident in Figures 9 and 10.

The comparative study for all instances is shown in Figures 11 and 12, which indicates both compressive and expansive waves for net volumetric cooling rate. From Figure 11, it is clear that in planar case, shock formation is early in comparison to cylindrically

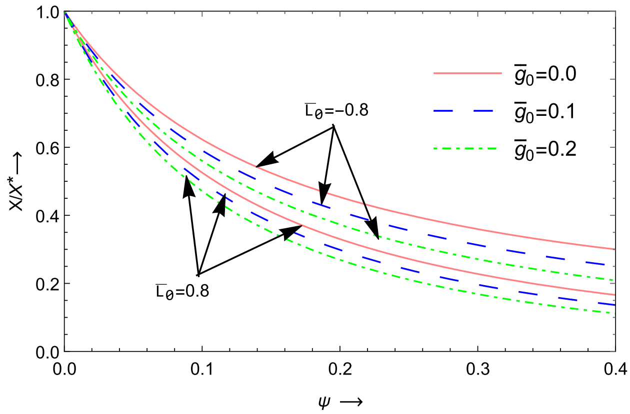

Figure 10. Effect of self gravitating parameter $\overline{g_0}$ for $\delta > 0$ with $\gamma = 1.67$, $\delta = 0.5$, $m = 2$ (spherical case) and $\bar{b} = 0.3$.

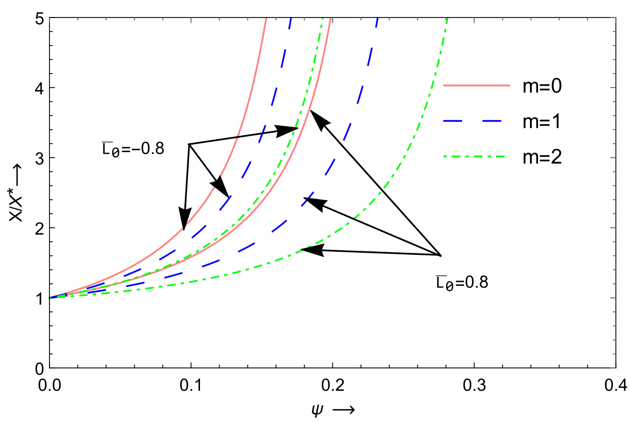

Figure 11. Comparative study of the geometry of non-ideal interstellar gas cloud for $\gamma = 1.67$, $\delta = -1.5$, $\bar{b} = 0.3$ and $\overline{g_0} = 0.5$.

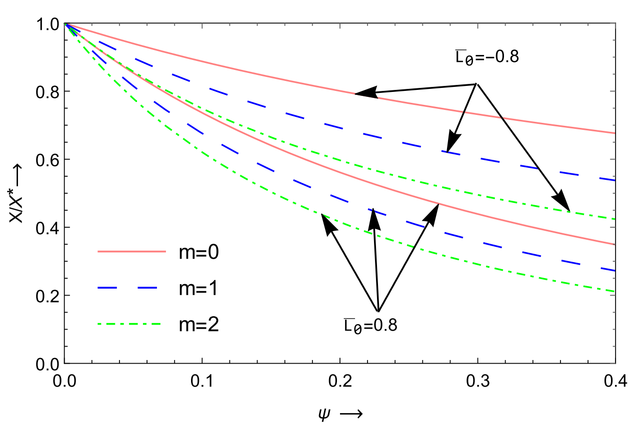

Figure 12. Comparative study of the geometry of non-ideal interstellar gas cloud for $\gamma = 1.67$, $\delta = 0.5$, $\bar{b} = 0.3$ and $\overline{g_0} = 0.5$.

and spherically symmetric cases. Clearly, compressive wave terminates into shock waves and expansion waves decays out.

5. Conclusions

This paper describes an analytical method to determine the solution of shocks for planar, cylindrical, spherical flows of hyperbolic system consisting of a one-dimensional inviscid, self-gravitating, non-ideal interstellar gas cloud. The propagation of weak discontinuity waves along the characteristics, are studied using the characteristic method. We found that expansive wave will exponentially decay in amplitude and will be damped out ultimately. The non-adiabatic and thermal behavior of the interstellar gas is the most important single factor influencing star formation. In the interiors of clouds that are effectively shielded from the galactic ultraviolet radiation field by interstellar grains. Molecular hydrogen is an important cooling agent. Self gravitation plays an important role in the fields of astronomy, seismology, geology and oceanography. The influence of self-gravitating parameter on shock formation is examined and we analyzed that it causes to accelerate the decay process of expansive waves and slows down the growth rate of compressive waves in the non-ideal interstellar gas cloud. Also, decaying of expansive wave is higher in the case of cooling gas cloud than that of heating gas cloud effect, and the growth of compressive wave is lower in case of cooling gas cloud than that of heating gas cloud effect. For cylindrically symmetric case, it is examined how the shock wave solution is influenced by the presence of van der Waals excluded volume and net volumetric cooling rate in the interstellar gas cloud. For more clarifications, a comparative study of planar and non-planar cases is done and it is observed that there is delay in the formation of shocks in spherically symmetric case shown in Figure 11.

Acknowledgements

The author, acknowledges Indian Institute of Technology, Banaras Hindu University, Varanasi, India for the award of institute fellowship. The authors are grateful to the anonymous referees for their valuable comments, which have helped to improve the manuscript.

References

Arora R., Siddiqui M. J. 2013, J. Theor. Appl. Phys., 7, 1
Arora R., Tomar A., Pal Singh V. 2012, Math. Model. Anal., 17, 351
Bedogni R., Woodward P. 1990, Astron. Astrophys., 231, 481

Bira B., Sekhar T. R., Sekhar G. R. 2018, Comput. Math. Appl., 75, 3873
Bisnovatyi-Kogan G., Silich S. 1995, Rev. Mod. Phys., 67, 661
Chaturvedi R. K., Singh L., *et al.* 2022, Chin. J. Phys.
Chaturvedi R. K., Srivastava S. K., Singh L. 2019, Eur. Phys. J. Plus, 134, 564
Chauhan A., Arora R. 2021, Math. Methods Appl. Sci., 44, 6282
Chen P. J., Gurtin M. E. 1971, Phys. Fluids, 14, 1091
Courant R., Friedrichs K. O. 1999, Supersonic Flow and Shock Waves, Vol. 21, Springer
Disney M., McNally D., Wright A. 1968, Mon. Notices R. Astron. Soc., 140, 319
Ferraioli F., Virgopia N. 1975, Memorie della Societa Astronomica Italiana, 46, 313
Ferraioli F., Ruggeri T., Virgopia N. 1978, Astrophys. Space Sci., 56, 303
Gupta B., Jena J. 2018, Int. J. Non-Linear Mech., 99, 51
Gupta P., Chaturvedi R. K., Singh L. 2020, Eur. Phys. J. Plus, 135, 1
Gupta N., Sharma K., Arora R. 2022, Math. Methods Appl. Sci., 45, 1259
Heathcote S., Brand P. 1983, Mon. Notices R. Astron. Soc., 203, 67
Higashino F. 1983, Zeitschrift für Naturforschung A, 38, 399
Hunter Jr. J. H. 1969, Mon. Notices R. Astron. Soc., 142, 473
Jena J., Mittal S. 2021, ANZIAM J., 63, 342
Lax P. D. 1957, Commun. Pure Appl. Math., 10, 537
Maslov V., Tsupin V. 1980, J. Sov. Math., 13, 163
Modelevsky E., Sari R. 2021, Phys. Fluids, 33, 056105
Nath G. 2020, J. Astrophys. Astron., 41, 1
Nath G. 2022, Zeitschrift für Naturforschung A
Nath G., Vishwakarma J. 2016, Acta Astronaut., 128, 377
Nath G., Singh S. 2019, J. Astrophys. Astron., 40, 1
Nath G., Sahu P., Chaurasia S. 2019, Chin. J. Phys., 58, 280
Ogino S., Tomisaka K., Nakamura F. 1999, Publ. Astron. Soc. Jpn., 51, 637
Pandey B. D. 1991, Zeitschrift Angewandte Mathematik und Mechanik, 71, 55
Pandey M., Sharma V. 2009, Q. Appl. Math., 67, 401
Roberts P., Wu C. 1996, Phys. Lett. A, 213, 59
Sahu P. 2022, Indian J. Phys., 1
Shah A., Saeed R., Noaman-ul Haq M. 2010, Phys. Plasmas, 17, 072307
Sharma K., Arora R. 2021, Ricerche di Matematica, 1
Shyam R., Sharma J., Sharma V. 1981, AIAA J., 19, 1246
Singh D., Arora R. 2021a, Math. Methods Appl. Sci., 44, 1514
Singh M., Arora R. 2021b, Phys. Fluids, 33, 046106
Singh L., Singh D., Ram S. 2016, Shock Waves, 26, 709
Singh M., Arora R., Chauhan A. 2020a, Ricerche di Matematica, 1
Singh M., Chauhan A., Sharma K., Arora R. 2020b, Phys. Fluids, 32, 107109
Srivastava S. K., Chaturvedi R. K., Singh L. 2020a, Phys. Scr., 95, 065205
Srivastava S. K., Chaturvedi R. K., Singh L. P. 2020b, Phys. Scr.
Srivastava S. K., Chaturvedi R. K., Singh L. P. 2021, Zeitschrift Naturforschung Teil A, 76, 435
Wu C., Roberts P. H. 1993, Phys. Rev. Lett., 70, 3424
Zeidan D., Pandey M., Govekar S. 2022, Phys. Fluids